Grading interfaces: a new concept to improve device performance in organic multilayer light-emitting diodes

Heike Riel, Siegfried Barth, Tilman A. Beierlein, Wolfgang Brütting, Siegfried Karg, P. Mueller, Walter Rieβ

Grading interfaces – A new concept to improve device performance in organic multilayer light-emitting diodes

H. Riel[a], S. Barth[a], T. Beierlein[a], W. Brütting[b], S. Karg[a], P. Müller[a], W. Rieß[a]

[a]IBM Research, Zurich Research Laboratory, CH-8803 Rüschlikon, Switzerland

[b]Experimental Physics II, University of Bayreuth, D-95440 Bayreuth, Germany

ABSTRACT

The influence of interfacial charges on the device characteristics of multilayer organic light-emitting diodes (OLEDs) is investigated, and a concept to improve device performance is presented. We studied devices consisting of copper phthalocyanine (CuPc) as hole injection and buffer layer, N, N'-di(naphthalene-1-yl)-N,N'-diphenyl-benzidine (NPB) as hole transport layer, and tris(8-hydroxyquinolinato)aluminum (Alq_3) as electron transport and emitting layer sandwiched between a high-work-function metal and a semi-transparent calcium electrode. Detailed current–voltage measurements show that the device characteristics in negative bias direction and at low positive bias below the built-in voltage depend strongly on the bias sweep direction, indicating that interfacial charges have a pronounced influence on the device characteristics. Low-frequency capacitance–voltage experiments reveal a voltage-independent capacitance in negative bias direction and a significant increase between 0 and 2 V, evidence of a redistribution of the internal electric field in this device configuration. Time-resolved electroluminescence (EL) measurements proved that also the EL response time at low voltages is governed by the accumulation of charge carriers inside the device rather than by their transport. Optimizing the device structure by grading the organic-organic interfaces results in an enhanced current flow, an improved brightness, and a faster EL response time. Our investigations clearly indicate that the abrupt CuPc-NPB as well as the NPB-Alq_3 interface significantly influence the performance of our multilayer OLED.

Keywords: OLED, space charges, graded interfaces, internal barriers, organic electroluminescence, organic multilayer light-emitting diodes

1. INTRODUCTION

The fabrication of efficient heterolayer organic light-emitting diodes (OLEDs) in 1987[1] has triggered substantial research activities worldwide in the field of organic electroluminescence (EL).[2] This huge interest is based on the fact that OLEDs fulfill all essential criteria for a flat-panel display (FPD): that they be lightweight, thin, have a wide viewing angle, high contrast ratio, low power consumption, video-rate response time, and full color availability. Owing to these intense experimental and also theoretical investigations, great progress has been achieved in fabricating more efficient and long-term-stable OLED devices. In the mean time, green-emitting OLEDs with luminous efficiencies of greater than 38 lm/W @ 100 cd/m^2 have been reported.[3] Similar progress has been achieved with regard to device lifetime, and various companies have demonstrated lifetimes exceeding 10,000 h to half brightness @ 100 cd/m^2 under constant current drive.[4] The best extrapolated values reported so far were by Eastman Kodak Co. with more than 90,000 h @ 100 cd/m^2 (Ref. 5). The temperature stability of the organic materials—also a crucial parameter in achieving long-term-stable OLEDs—has significantly improved, and materials with a glass temperature of $\geq$ 130 $°$C have become commercially available.[6] Moreover, passively and even actively driven organic EL displays with impressive device performance have been presented.[7]

For display applications, especially for active matrix addressing, the operating voltage should be as low as possible. In the past years tremendous progress has been achieved in reducing the voltage mainly by optimizing and modifying the electrodes[8-10] and by using new concepts for charge-carrier injection, such as inorganic injection layers[11-14] and inorganic/organic multilayer device structures.[15] Besides the energy barriers at the charge-carrier-injecting electrodes, also the barriers between adjacent organic layers of a multilayer OLED may influence the device characteristics. These internal barriers, together with the different charge carrier mobilities in contiguous organic layers, lead to interfacial space charge formation. Consequently, the applied electrical field is screened, resulting in a flatter device characteristic and a reduced current flow at a given voltage. On the other hand, space charges may also lead to an enhanced degradation of the OLED. Therefore it is essential to understand the critical interfaces and to reduce or even prevent space charges by thorough device

design. Recently we introduced a simple concept of graded interfaces between adjacent organic layers to improve the performance of multilayer OLEDs.[16]

Here we will present further, detailed investigations of the influence of interfacial charges on the device characteristics of multilayer OLEDs, including low-frequency capacitance–voltage and transient EL measurements, and prove that the grading concept is appropriate. The graded interfaces significantly enhance current flow and brightness, and result in a faster EL response time compared to conventional OLED structures at the same voltage.

2. EXPERIMENTAL AND DEVICE STRUCTURES

The OLEDs were built on glass substrates (Schott AF 45) precoated with an opaque high-work-function metal anode. The organic multilayer structure consists of copper phthalocyanine (CuPc), N,N'-di(naphthalene-1-yl)-N,N'-diphenyl-benzidine (NPB), and tris(8-hydroxy-quinolinato) aluminum (Alq$_3$) with typical thicknesses of 20, 45, and 60 nm, respectively, and a thin calcium (Ca) cathode on top. In this device configuration the EL is observed through the semitransparent cathode. The active area of our devices was 2×3 mm^2. The schematic energy level diagram and the molecular structure of the organic materials used are shown in Figure 1.
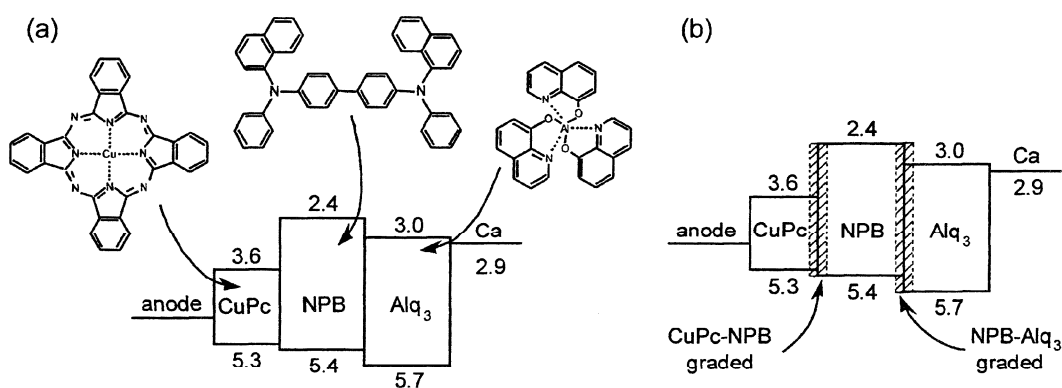

Figure 1. Schematic energy-level diagrams and molecular structures of the organic materials used: (a) of a conventional OLED, and (b) of an OLED with graded interfaces (typical width of grading zone: 10 nm).

Prior to use, all organic materials were purified by vacuum sublimation. Depositions were carried out in a high-vacuum system (Leybold) by thermal evaporation from resistively heated tantalum and tungsten boats. The base pressure in the chamber ranged between 4×10^{-7} and 1×10^{-6} mbar. A typical deposition rate for the organic compounds and the metal was $\cong 1$ Å/s. Graded interfaces of the various organic layers were obtained by coevaporation. Deposition rates were individually controlled by calibrated quartz-crystal monitors. As the evaporation system is equipped with a rotating sample holder and a specially designed shutter mechanism, three devices can be fabricated simultaneously and controlled independently. This enables side-by-side comparison of OLEDs differing in only one parameter, whereby uncertainties as would result from different evaporation processes are avoided. The growth chamber is attached directly to a glovebox system filled with argon, which allows devices to be fabricated, characterized, and encapsulated under inert conditions.

Current–voltage (I–V) and brightness–voltage (EL–V) characteristics were measured with a Hewlett Packard parameter analyzer (HP 4145B) and a sensitive silicon photodiode (Hamamatsu S2281). The luminance calibration of the photodiode was obtained with a Photo Research PR704 spectroradiometer. Transient EL was measured in a specially designed setup that allows the simultaneous detection of time-dependent EL as well as current and voltage across the device. The OLEDs were characterized in a modified HP 16058A test fixture with a Hamamatsu photomultiplier 5783-01 (time resolution $\cong$ 0.65 ns) located directly on top of the emitting area to detect EL intensity. A HP 8116A DC pulse/function generator (50 MHz, rise time $\cong$ 7 ns, decay time $\cong$ 10 ns) was used to apply rectangular voltage pulses to the device. The pulse length was varied between 150 and 800 μs with a duty cycle of 10%. The function generator permits the OLED to be driven with various positive and negative offset voltages before the rectangular voltage pulses are applied. The photomultiplier was connected to the 50-Ω input resistance of a digital oscilloscope (Tektronix 2440) to record the EL signal. A second digital oscilloscope

(Tektronix 2440) allows the voltage pulse and the time-dependent current flow through the device to be monitored simultaneously with the EL signal. Capacitance–voltage (C–V) measurements were carried out with a frequency response analyzer (Solartron Instruments SI1260). Typically, the oscillator level was set to 50 mV, and the measurement averaged over 100 cycles of the respective frequencies. All measurements were carried out with encapsulated devices at room temperature.

3. RESULTS AND DISCUSSION

Figure 2 presents the dependence of the I–V and EL–V characteristics on the bias sweep direction for a multilayer OLED consisting of a metal anode/CuPc (20 nm)/NPB (45 nm)/Alq$_3$ (65 nm)/Ca cathode. To reveal the influence of different sweep directions on the device characteristics, the data are presented in a semi-logarithmic plot. The voltage sweep was from −5 to 10 V and back again, in steps of 50 mV. Current and brightness were detected with the parameter analyzer set to medium integration time and the delay time between individual data points to 0 s. In this mode the acquisition time for a single data point depends on the magnitude of the detected current, and ranges from 10 to 100 ms for the given device. In forward bias direction the current increases strongly above a threshold voltage of 2.0 V, and is virtually unaffected by the sweep direction (Figure 2). The onset of EL determined at 0.1 mcd/m^2 is 2.1 V, and it is not affected by external, i.e. measurement, parameters. We note that the onset voltage for detectable EL is significantly lower than the optical gap of Alq$_3$ (2.7 eV) and corresponds approximately to the built-in voltage (i.e. the difference in work function) of the two electrodes. Remarkable differences in the current flow are observed below 2.0 V. In this voltage range only one type of charge carriers (holes) is injected and thus no EL is detectable. In addition a strong dependence on the measurement direction is observed. Specifically, the voltage at which the current passes through zero is not at zero bias but at about −0.8 V for increasing voltage and at about +1.9 V for the other sweep direction. This hysteresis of the I–V characteristics is a clear indication of the presence of space charges in the device, which may result from the existence of deep traps in these materials[17] and/or an accumulation of charge carriers at internal energy barriers. As the observed phenomena occur mainly in the voltage range where only holes are injected into our multilayer OLED, the energy barriers between CuPc and NPB as well as between NPB and Alq$_3$ can be responsible for these effects. Furthermore, under the above measurement conditions, a step-like structure is observed at ≅1.0 V in the "−" to "+" sweep direction, which we found to be characteristic for a multilayer structure containing CuPc. We do not observe this feature if the CuPc layer is omitted.
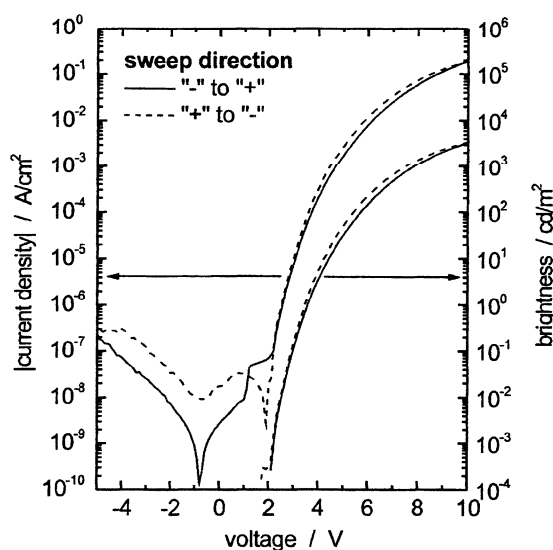

Figure 2. Current–voltage and brightness–voltage characteristics of an anode/CuPc (20 nm)/NPB (45 nm)/Alq$_3$ (60 nm)/Ca OLED measured in different sweep directions with identical data acquisition time.

Figure 3 shows the capacitance as a function of frequency for various applied bias values (Figure 3a) and as a function of bias for a fixed frequency of 10 Hz (Figure 3b). The frequency-dependent measurements reveal that at zero and negative bias the capacitance is essentially frequency-independent up to some 10^4 Hz, having a value of about 2 nF. This value corresponds to the geometrical capacitance of the device when taking into account a dielectric constant for the organic
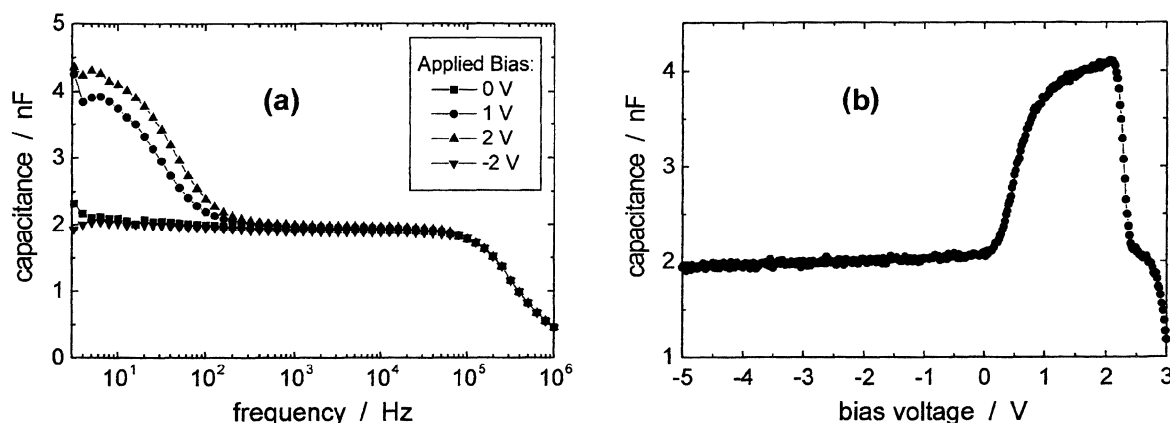
Figure 3. Dependence of the capacitance on (a) the frequency and (b) the voltage of the OLED in Figure 2.

materials of 3.5. Above 10^5 Hz the capacitance drops rapidly to a value much lower than the one corresponding to the materials' dielectric constants. This can be ascribed to parasitic effects due to lead/contact resistances and capacitances, which will not be discussed further here. The frequency dependence of the capacitance is almost identical for all applied bias values above about 200 Hz. Below 200 Hz and for positive bias (1 and 2 V), an increase in the capacitance is observed. At low frequencies ($f < 10$ Hz) the capacitance seems to saturate at a value independent of the bias. To study the bias dependence in more detail, the applied bias was varied at a fixed frequency of 10 Hz (Figure 3b). This frequency is in most cases sufficiently low to monitor the saturation value of the capacitance, and still yields a good signal-to-noise ratio. The data shown in Figure 3b were taken from –5 to 3 V in steps of 25 mV with an additional delay of 10 s between the individual data points. No difference was observed for the opposite sweep direction. Whereas there is only a very weak bias dependence in the negative direction, the capacitance increases significantly for positive bias at about 0.2 V and reaches a maximum at 2.1 V, which coincides with the onset of EL (Figure 2). Above this voltage the capacitance decreases sharply to a value of about 2 nF before it finally drops further as the bias exceeds 2.5 V. Note that in the regime of double carrier injection accompanied by recombination, the capacitance is not well-defined and thus no measurements for voltages above 3 V have been performed. From the $C–V$ measurements in Figure 3b we can see that there is a transition from a situation in which the capacitance is equal to the geometrical capacitance of the device for $V < 0$ V to one for V approaching 2 V (in this device configuration) where the capacitance is now about twice as large as in reverse bias direction. This corresponds well to the thickness of the Alq$_3$ layer of 60 nm compared to about 65 nm for the sum of the CuPc and NPB layer thicknesses. By systematic variation of both organic layer thicknesses on ITO/NPB/Alq$_3$/Ca devices[18] it was found that the value of the capacitance in reverse bias direction always corresponds to the total thickness of all organic layers, whereas the value at 2 V is solely determined by the thickness of the Alq$_3$ layer. Moreover, the increase in the capacitance at a voltage well below the built-in voltage ($V_{bi} \cong 2$ V) was explained by the presence of negative interfacial charges at the NPB/Alq$_3$ interface resulting in a discontinuity of the electric field. Our $C–V$ measurements also prove that under a sufficiently large negative bias the OLED actually behaves like a dielectric with no mobile charges inside the organic layers. The weak voltage dependence of the capacitance observed in this range can be attributed to the presence of the CuPc layer (presumably some residual doping) and is not seen if this layer is omitted. When the bias voltage is increased above 0 V, the capacitance increases, indicating that the NPB layer has reached the flat-band condition and its resistance drops drastically.[18] With increasing bias, holes are injected from the anode and gradually reduce immobile negative charges at the NPB/Alq$_3$ interface until at V_{bi} the negative interfacial charge is fully compensated, and the device is in the flat-band condition.

Figure 4 demonstrates the typical time-resolved EL response of our conventional OLED upon application of a rectangluar voltage pulse with an amplitude of 4 V and two different offset voltages of 0 and 2 V. The EL signals are characterized by a finite delay time between the application of the voltage pulse and the first appearance of EL, an extrapolated rise time to reach a steady-state value, and finally the plateau value itself. It is common practice to interpret the onset of EL in single-layer devices as the transit time of the majority charge carriers.[19] However, the mobility values obtained via the EL response time from single-, double- as well as multi-layer OLEDs have been found to be orders of magnitudes lower than those determined from time-of-flight (TOF) measurements, especially at low voltages.[20-22] After the application of a rectangular voltage pulse, several processes have to occur before light emission can be observed from multilayer OLEDs: injection of holes at the anode and buildup of positive space charges at the NPB/Alq$_3$ interface, injection of electrons at the cathode and
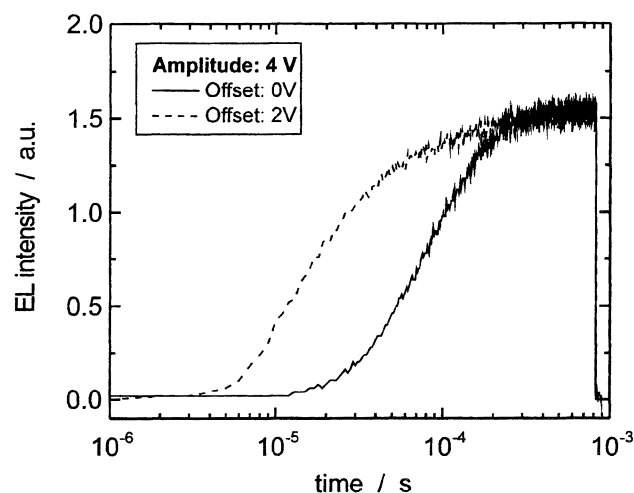
Figure 4. Comparison of the time response of EL from an anode/CuPc (20 nm)/NPB (45 nm)/Alq$_3$ (60 nm)/Ca device upon application of two different offset voltages (0 and 2 V) before application of an 800-μs-long rectangular voltage pulse with an amplitude of 4 V and a duty cycle of 10%.

transport of electrons to the NPB/Alq$_3$ interface, where they can ultimately recombine radiatively with holes injected from the NPB into the Alq$_3$ layer. Therefore it is not quite that straightforward to obtain charge-carrier mobilities from the delayed onset of EL observed in the time-resolved EL experiment of our multilayer OLED. An important question is whether the observed EL response times are dominated by electron transport through the Alq$_3$ layer to the recombination zone or result from the buildup of the internal space charge and the concomitant redistribution of the electric field inside the device. A direct check whether the buildup of space charges contributes to the observed temporal response of the OLED can be obtained by superimposing a DC offset bias to the applied voltage pulse. Figure 4 compares two EL traces obtained with the same voltage amplitude of 4 V but different offset biases: 0 and 2 V. The bias value of 2 V is chosen just below the onset of double carrier injection to guarantee that negative charges at the NPB/Alq$_3$ interface are compensated, as has been proved by the C–V measurements (Figure 3). Figure 4 clearly shows that the delay and rise times of the EL signal to a steady-state value are at least a factor of 2 shorter if a positive bias of 2 V is applied prior to application of the 4-V voltage pulse, which directly proves that in this OLED structure the buildup of space charges has a significant influence on the temporal response of light emission.

To monitor the influence of the internal energy barriers on the device characteristics of our OLEDs, we prepared devices with graded interfaces and compared them with the conventional diode structure (Figure 5). The I–V and EL–V curves were detected with identical parameters starting at –5 V. Apart from slight variations in the zero crossing of the current, the devices show almost identical behavior in reverse direction. Moreover, their onset voltages for EL (2.1 V) are more or less identical. However, above this threshold voltage the OLEDs with graded interfaces show much steeper characteristics and therefore a higher current flow accompanied by an enhanced brightness at a given voltage. For example, whereas the conventional structure requires 6.0 V to obtain 100 cd/m^2, the CuPc-NPB graded device needs only 5.0 V. The steeper characteristics of the OLEDs with mixed interfaces can result from several effects. First, the regions where charge carriers can accumulate are smeared out, and therefore the internal space charge is redistributed, leading to a modified internal electrical field distribution and thus to an enhanced probability for holes to enter the adjacent layer. Additionally, owing to the disorder in the graded regions, the density of states of both organic materials is broadened, facilitating charge-carrier injection. Consequently the influence of the internal energy barriers is reduced, resulting in significantly steeper I–V and EL–V characteristics. When comparing the two graded OLEDs, it is conspicuous that the CuPc-NPB graded device shows the steeper I–V characteristic and the higher brightness. Moreover, whereas the pronounced structure between 0 and 2 V is observed in both the conventional and the NPB-Alq$_3$ graded OLED, it is clearly reduced in the CuPc-NPB graded device.

This pronounced influence of the CuPc-NPB graded interface is also noticeable on the EL response, see Figure 6. The comparison between the conventional OLED and the graded CuPc-NPB device clearly proves the faster EL response and rise times of the latter. Obviously the grading of the interface leads to an improved injection and transport through the various organic layers and interfaces, and concomitantly to a higher brightness at a given voltage.
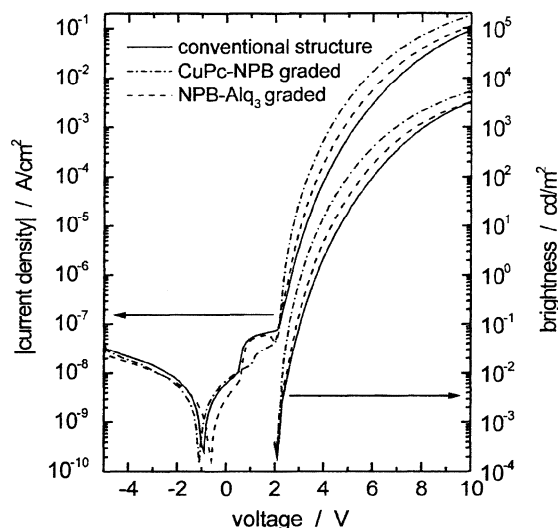
Figure 5. Comparison of the current–voltage and brightness–voltage characteristics of three multilayer OLEDs that differ in only one parameter. Their structures are anode/CuPc (20 nm)/NPB (45 nm)/Alq$_3$ (60 nm)/Ca, anode/CuPc/NPB/NPB:Alq$_3$/Alq$_3$/Ca, and anode/CuPc/CuPc:NPB/NPB/ Alq$_3$/Ca. The sweep direction was the same for all three devices ("–" to "+").
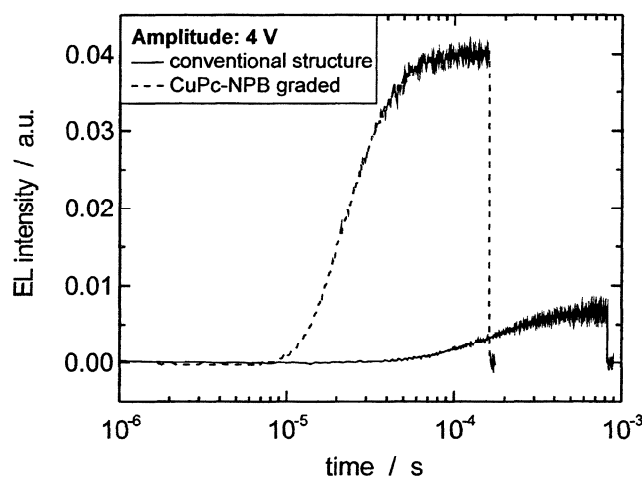

Figure 6. Comparison of the transient EL signal from an conventional OLED (anode/CuPc (20 nm)/ NPB (45 nm)/Alq$_3$ (60 nm)/Ca) and an CuPc-NPB graded device (anode/CuPc/CuPc:NPB/NPB/Alq$_3$/Ca) upon application of a rectangular voltage pulse with an amplitude of 4 V and a pulse width of 150 and 800 μs, respectively. The duty cycle was 10% in both cases.

Finally, it is expected that graded interfaces stabilize OLEDs, i.e. lead to doping of the hole-transport layer[23] or to mixed emitting layers of hole- and electron-transporting molecules,[24,25] resulting in a reduced intrinsic device degradation and hence in an improved device lifetime. Such lifetime measurements are currently under way.

4. CONCLUSION

We have presented a brief overview of our current studies on the influence of interfacial charges on the device characteristics of conventional multilayer (anode/CuPc/NPB/Alq$_3$/Ca) OLEDs. These experiments include current–voltage, current–brightness, low-frequency capacitance–voltage as well as time-resolved electroluminescence measurements. We

were able to establish the concept of graded interfaces as an excellent method to improve device performance in multilayer devices. Additionally, the EL response and rise times are dramatically shortened by grading the interfaces. Our investigations have especially shown that positive space charges at the CuPc-NPB interface limit injection into the adjacent NPB layer. Therefore internal barriers rather than charge-carrier transport restrict the current flow and determine the device characteristics of our OLED multilayer structure at low voltages.

ACKNOWLEDGMENTS

REFERENCES

1. C. W. Tang and S. A. VanSlyke, "Organic electroluminescent diodes," *Appl. Phys. Lett.* **51**, p. 913 (1987).
2. See, for example, Proc. 2nd Int'l Conf. on Electroluminescence of Molecular Materials and Related Phenomena, Sheffield, UK, May 1999, in *Synth. Met.* **111-112**, pp. 1-622 (2000), and references therein.
3. T. Tsutsui, M.-J. Yang, M. Yahiro, K. Nakamura, T. Watanabe, T. Tsuji, Y. Fukuda, T. Wakimoto, and S. Miyaguchi, "High-quantum efficiency in organic light-emitting devices with iridium-complex as a triplet emissive center," *Jpn. J. Appl. Phys.* **38**, p. L1502 (1999).
4. See, for example, Stanford Resources Inc., *Organic Light-Emitting Diodes (OLEDs) –Technology Trends and Display Market Assessment*, San Jose, CA, 2000.
5. C. W. Tang, private communication.
6. H. Spreitzer, H. Schenk, J. Salbeck, F. Weissörtel, H. Riel, and W. Rieß, "Temperature stability of OLEDs using amorphous compounds with spiro-bifluorene core," in *Proc. SPIE Int'l Conf. on Organic Light-Emitting Materials and Devices III*, Denver, CO, July 1999, Proc. SPIE **3797**.
7. SANYO Electric and Kodak Eastman Co.: "World's largest full-color OLED-Display – 5.5-Inch QVGA LT-p-Si TFT AM-OLED," Special demonstration at the Int'l Society for Information Display's SID 2000 Conference, May 14-19, 2000, Long Beach, CA.
8. T. Wakimoto, S. Kawani, K. Nagayama, Y. Yonemoto, R. Murayama, J. Funaki, H. Sato, H. Nakada, and K. Imai, "Organic EL cells with high luminous efficiency, " in *Technical Digest of the Int'l Symp.on Inorganic and Organic Electroluminescence*, Hamamatsu, 1994, p. 77.
9. S. Fujita, T. Sakamoto, K. Ueda, K. Ohta, and S. Fujita, "Surface treatment of indium-tin-oxide substrates and its effects on initial nucleation processes of diamine films," *Jpn. J. Appl. Phys.* **36**, p. 350 (1997).
10. A. Berntsen, P. Van de Weijer. Y. Croonen. C. Liedenbaum, and J. Vleggaar, "Degradation mechanisms of polymer LEDs," in *Conference Record of the 17th Int'l Display Research Conference, Society for Information Display*, J. Morreale (Ed.), Santa Ana, CA, 1997, p. F-28.
11. M. Meier, M. Cölle, S. Karg, E. Buchwald, J. Gmeiner, W. Rieß, and M. Schwoerer, "Metal/insulator/polymer LEDs based on PPV," *Mol. Cryst. Liq. Cryst.* **283**, p. 197 (1996).
12. L. S. Hung, C. W. Tang, and M. G. Mason, "Enhanced electron injection in organic electroluminescent devices using an Al / LiF electrode," *Appl. Phys. Lett.* **70**, p. 152 (1997).
13. F. G. Celii and S. J. Jacobs, "High efficiency organic LEDs", in *Conference Record of the 17th Int'l Display Research Conference, Society for Information Display*, J. Morreale (Ed.), Santa Ana, CA, 1997, p. 314.
14. G. E. Jabbour, Y. Kawabe, S. E. Shabeen, J. F. Wang, M. M. Morrel, B. Kippelen, and N. Peyghambarian, "Highly efficient and bright organic electroluminescence devices with an aluminum cathode," *Appl. Phys. Lett.* **71**, p. 1762 (1997).
15. W. Rieß, H. Riel, P. F. Seidler, and H. Vestweber, "Organic-inorganic multilayer structures: a novel route to highly efficient organic light-emitting diodes," *Synth. Met.* **99**, p. 213 (1999).
16. H. Riel, W. Brütting, T. Beierlein, E. Haskal, P. Müller, and W. Rieß, "Influence of space charges on the current-voltage characteristics of organic light-emitting devices," *Synth. Met.* **111-112**, p. 303 (2000).
17. S. Karg, J. Steiger, and H. von Seggern, "Determination of trap energies in Alq_3 and TPD," *Synth. Met.* **111-112**, p. 277 (2000).
18. S. Berleb, W. Brütting, and G. Paasch, "Interfacial charges and electric field distribution in organic heterolayer light-emitting devices," submitted to *Organic Electronics* (2000).
19. See, for example, H. Vestweber, J. Oberski, A. Greiner, W. Heitz, R. F. Mahrt, and H. Bässler, "Electroluminescence from phenylenevinylene-based polymer blends," *Adv. Mat. Optics and Electron.* **2**, p. 197 (1993).

20. P. Delannoy, G. Horowitz, H. Bouchriha, F. Deloffre, J.-L. Fave, F. Garnier, R. Hajlaoui, M. Heyman, F. Kouki, J.-L. Monge, P. Valat, V. Wintgens, and A. Yassar, "Transient electroluminescence of monolayer and bilayer sexithiophene diodes," *Synth. Met.* **67**, p. 197 (1994).

21. S. Karg, V. Dyakonov, M. Meier, W. Rieß, and G. Paasch, "Transient electroluminescence in poly(p-phenylenevinylene) light-emitting diodes," *Synth. Met.* **67**, p. 165 (1994).

22. Y.-H. Tak, H. Vestweber, H. Bässler, A. Bleyer, R. Stockmann, and H.-H. Hörhold, "Time-resolved electroluminescence from single and bilayer LEDs based upon substituted poly-arylenes," *Chem. Phys.* **212**, p. 471 (1996).

23. Y. Hamada, T. Sano, K. Shibata, and K. Kuroki, "Influence of the emission site on the running durability of organic electroluminescent devices," *Jpn. J. Appl. Phys.* **34**, p. L824 (1995).

24. Z. D. Popovic, H. Aziz, C. P. Tripp, N.-X. Hu, A.-M. Hor, and G. Xu, "Improving the efficiency and stability of organic light-emitting devices by using mixed emitting layers," in *Proc. SPIE Int'l Conf. on Organic Light-Emitting Materials and Devices II*, San Diego, CA, July 1998, *Proc. SPIE* **3476**, p. 68.

25. H. Aziz, Z. D. Popovic, N.-X. Hu, A.-M. Hor, and G. Xu, "Degradation mechanism of small molecule-based organic light-emitting devices, " *Science* **283**, p. 1900 (1999).